Critical Interactions in Binding Antibody NC41 to Influenza N9 Neuraminidase: Amino Acid Contacts on the Antibody Heavy Chain†

Pamela S. Pruett‡,§ and Gillian M. Air*,||

Department of Microbiology, University of Alabama at Birmingham, Birmingham, Alabama 35294, and Department of Biochemistry and Molecular Biology, University of Oklahoma Health Sciences Center, Oklahoma City, Oklahoma 73190

Received January 27, 1998; Revised Manuscript Received April 27, 1998

ABSTRACT: Antibody NC41 binds to the subtype N9 neuraminidase (NA) of influenza virus A/tern/Australia/G70c/75 and inhibits its enzyme activity. To address the molecular mechanisms by which antibodies interact with neuraminidase and the requirements for successful escape from antibody inhibition, we made amino acid substitutions in heavy chain CDRs of NC41. Antibody proteins expressed as a single-chain Fv (scFv) fused with maltose-binding protein were assayed for binding to NA by ELISA. Association constants (K_a) for wild-type and mutant scFvs are as follows: wild type, 2×10^7 M^{-1}; Asn31 → Gln, 2×10^7 M^{-1}; Glu96 → Asp, 1×10^7 M^{-1}; Asp97 → Lys, 6×10^6 M^{-1}; and Asn98 → Gln, 8×10^6 M^{-1}. The K_a for intact NC41 antibody was 4×10^8 M^{-1} in the same assay, reflecting increased stability compared to that of the scFv. Mutations in the scFv antibody had less of an effect on binding than mutations in their partners on the NA, and modeling studies suggest that interactions involving the mutant antibody side chains occur, even without taking increased flexibility into account. Asp97 forms a salt link with NA critical contact Lys434; of the four mutants, D97K shows the largest reduction in binding to NA. Mutant N98Q also shows reduced binding, most likely through the loss of interaction with NA residue Thr401. Substitution N31Q had no effect on K_a. NC41 residue Glu96 interacts with NA critical contact Ser368, yet E96D showed only a 2-fold reduction in binding to NA, apparently because the H bond can still form. Asp97 and Asn98 provide the most important interactions, but some binding is maintained when they are mutated, in contrast to their partners on the NA. The results are consistent with maturation of the immune response, when the protein epitope is fixed while variation in the antibody paratope allows increasing affinity. Influenza viruses may exploit this general mechanism since single amino acid changes in the epitope allow the virus to escape from the antibody.

Although it has been the subject of intense biomedical and clinical research, influenza continues to have a major health impact in the United States, as well as in the rest of the world. Especially susceptible are the elderly, infants, immunosuppressed patients, and those with other respiratory ailments. Pneumonia and influenza are the sixth leading cause of death in the United States (*1*).

Influenza viruses belong to the family Orthomyxoviridae and contain a segmented, negative sense, single-stranded RNA genome. The ability of influenza virus to change its antigenic structure enables it to escape the host's immune system. These changes occur in the two major surface glycoproteins: (1) hemagglutinin (HA[1]), which binds to sialic acid receptors, and (2) neuraminidase (NA), which cleaves sialic acid and facilitates the release and spread of the virus (*2*, *3*). Vaccines have not been effective in controlling the recurring epidemics of influenza because of variation in these surface antigens.

One step in understanding the mechanism by which the influenza virus escapes from antibodies is determination of the crystal structure of the glycoprotein antigens complexed with monoclonal antibodies. This is the only way in which epitopes can be unambiguously characterized. Mapping of antigenic sites by generation of virus escape mutants grown in the presence of neutralizing antibodies and the determination of amino acid changes give a very incomplete view of the epitope. In the epitope on G70c NA recognized by antibody NC41, the most important contacts on the antigen were identified by escape mutant analysis (*4*), but the complete epitope involves 16 other amino acids (*5*).

Considerable effort has been put forth to understand the mechanism by which antibodies bind specifically to antigen with high affinity yet great specificity. Antibody diversity

† This work was supported in part by Grant AI-19084 from the National Institute of Allergy and Infectious Diseases.

* To whom correspondence should be addressed: Department of Biochemistry and Molecular Biology, University of Oklahoma Health Sciences Center, P.O. Box 26901, Oklahoma City, OK 73190. Phone: (405) 271-2227, ext. 1250. Fax: (405) 271-3205. E-mail: gillian-air@ouhsc.edu.

‡ University of Alabama at Birmingham.

§ Present address: Institute of Molecular Biophysics, Florida State University, MBB459L, Tallahassee, FL 32306.

|| University of Oklahoma Health Sciences Center.

[1] Abbreviations: NA, neuraminidase; ELISA, enzyme-linked immunosorbent assay; HA, hemagglutinin; CDR, complementarity-determining region; scFv, single-chain Fv domain of antibody; NWS-G70c, reassortant virus A/NWS/33_{HA}-tern/Australia/G70c/75_{NA}; PCR, polymerase chain reaction; AbL, antibody linker, $(Gly_4Ser)_3$; MBP, maltose-binding protein; ABTS, 2,2′-azinobis(3-ethylbenzthiazoline-6-sulfonic acid).

S0006-2960(98)00205-0 CCC: $15.00
Published on Web 07/09/1998

Table 1: Buried Surface and Contacts in Antigen−Antibody Complexes[a]

		antigen in complex			antibody in complex			complex			
antigen	antibody	buried surface (Å^2)	no. of contacts	no. of loops	buried surface (Å^2)	no. of contacts	CDRs in contact	H bonds	vdW contacts	salt links	buried H_2O's
lysozyme											
HEL	D1.3 (*35*)	748	12	2	680	12	6	20	75	0	3
HEL	HyHEL-10 (*36*)	774	15	4	720	19	6	14	111	1	0
HEL	HyHEL-5 (*37*)	750	13	3	750	16	6	14	74	3	0
PHL	D11.15 (*38*)	681	10	3	648	12	4	5		2	
antibody											
FvE5.2	FvD1.3 (*39*)	974	17	6	912	18	6	12			
Fab225	FabD1.3 (*40*)	800	15	6	800	13	5	9		1	
staphylococcal nuclease	N10 (*41*)	828	17	5	793	18	6	7	102	2	
neuraminidase	NC41 (*5*)	899	19	5	916	17	5	12	104	1	0
	NC10 (*42*)	716	15	4	697	14	4	12		0	3

[a] Structures refined to better than 3 Å are included. Some of this information was previously compiled (*32*−*34*).

is manifested in the antigen-combining regions, the six "complementarity-determining regions" [CDRs (*6*)], three on the heavy chain (H1−3) and three on the light chain (L1−3). Despite their sequence diversity, five of the six CDRs assume a limited number of conformations, the canonical structures (*7*). CDR H3 is formed by the D and J genes brought together during VDJ rearrangement and has little or no sequence conservation or common structural motifs and, therefore, has no canonical structures. In many crystal structures of protein−Fab complexes, CDR H3 contributes significantly to binding interactions, and thus, its variability and flexibility contribute significantly to antibody diversity (*8*).

The properties of the higher-resolution antibody−protein complex crystal structures are compared in Table 1. These complexes involve two to five polypeptide loops in the protein interacting with four to six antibody CDRs. All the epitopes are highly conformation dependent. Complex formation involves 12−19 amino acids on each interacting protein, with 12−20 hydrogen bonds, 0−3 salt links, 75−111 van der Waals contacts, and 1400−1800 Å^2 of total buried surface area. Most antibody−protein structures to date show "lock and key" surface and chemical complementarity, exhibiting little change in the conformation of either component upon binding. One exception is CDR3 of the HC19 Fab heavy chain, which moves 10 Å upon binding to HA (*9*). At a medium resolution of 3.3 Å, this complex is similar in character to those shown in Table 1, on the basis of its total buried surface area of 1250 Å^2 in the interface and its use of 10 hydrogen bonds. NC41 has not been crystallized by itself so it is not known if there are changes in the bound versus unbound state of the antibody, but no dramatic changes are seen in the bound versus unbound state of the neuraminidase (*10*).

Escape mutants of G70c NA were generated by growth of reassortant influenza virus A/NWS/33$_{HA}$-tern/Australia/G70c/75$_{NA}$ (NWS-G70c) in the presence of NC41 (*11*). Monoclonal antibody NC41 binds to an epitope on the rim of the enzyme active site of G70c NA (Figure 1). Sequence analysis of 19 independently selected escape mutants showed that, except for one double mutant, only a single amino acid was changed and there were only four sites of change, defining residues 368, 373, 400, and 434 as being important to the interaction (*11*, *12*). The NC41 epitope was definitively mapped by X-ray crystal structure determination of the Fab−NA complex refined to 2.9 Å resolution (*5*). When the NC41 epitope was examined by site-directed mutagenesis of the NA, it was found that, of the 19 amino acids in contact with NC41, only the side chains of Ser368, Asn400, and Lys434 were critical to the interaction, in that even very conservative substitutions abrogated binding (*4*).

The interface between NC41 and G70c NA has excellent surface and chemical complementarity. The NC41 epitope on G70c NA is comprised of five polypeptide segments on four loops surrounding the enzyme active site and is discontinuous, like all other structurally defined epitopes on native proteins (*13*). The chemical complementarity involves one buried salt bridge and twelve hydrogen bonds, with additional van der Waals interactions (*5*, *14*). These interactions involve 19 residues on five polypeptide segments of G70c NA in contact with 17 residues in five of the six NC41 CDRs. A ridge in NC41 CDR H3 made of residues Glu96, Asp97, and Asn98 fits into a groove on the NA formed by residues 368−373 and 400−403 with NA residue Lys434 making a salt bridge with AspH97.

To test if critical contacts on the NA are paired with critical contacts on the antibody, we made the following mutations in the heavy chain of NC41: Asn → Gln at position 31 (N31Q, interacts with critical contact Asn400), Glu → Asp at position 96 (E96D, side chain interacts with critical contact Ser368), Asp → Lys at position 97 (D97K, forms salt link with critical contact Lys434), and Asn → Gln at position 98 (N98Q, provides two of the twelve hydrogen bonds between the antibody and NA). Together, these residues form nine of the twelve hydrogen bonds of the Fab−NA complex, as well as the only salt bridge (Figure 2). The effect of these mutations on the ability of the antibody to bind G70c NA was determined by ELISA. The analysis of the individual contributions of antibody amino acid residues in the paratope to the strength of the binding interaction provides insight into the mechanisms by which antibodies recognize and bind antigen.

MATERIALS AND METHODS

Viruses. Influenza contains an RNA genome, comprised of eight segments. Within a mixed infection, one or more of these segments can be exchanged between strains and incorporated into virions, creating a "reassortant" virus. The influenza strain used was a reassortant virus made to facilitate

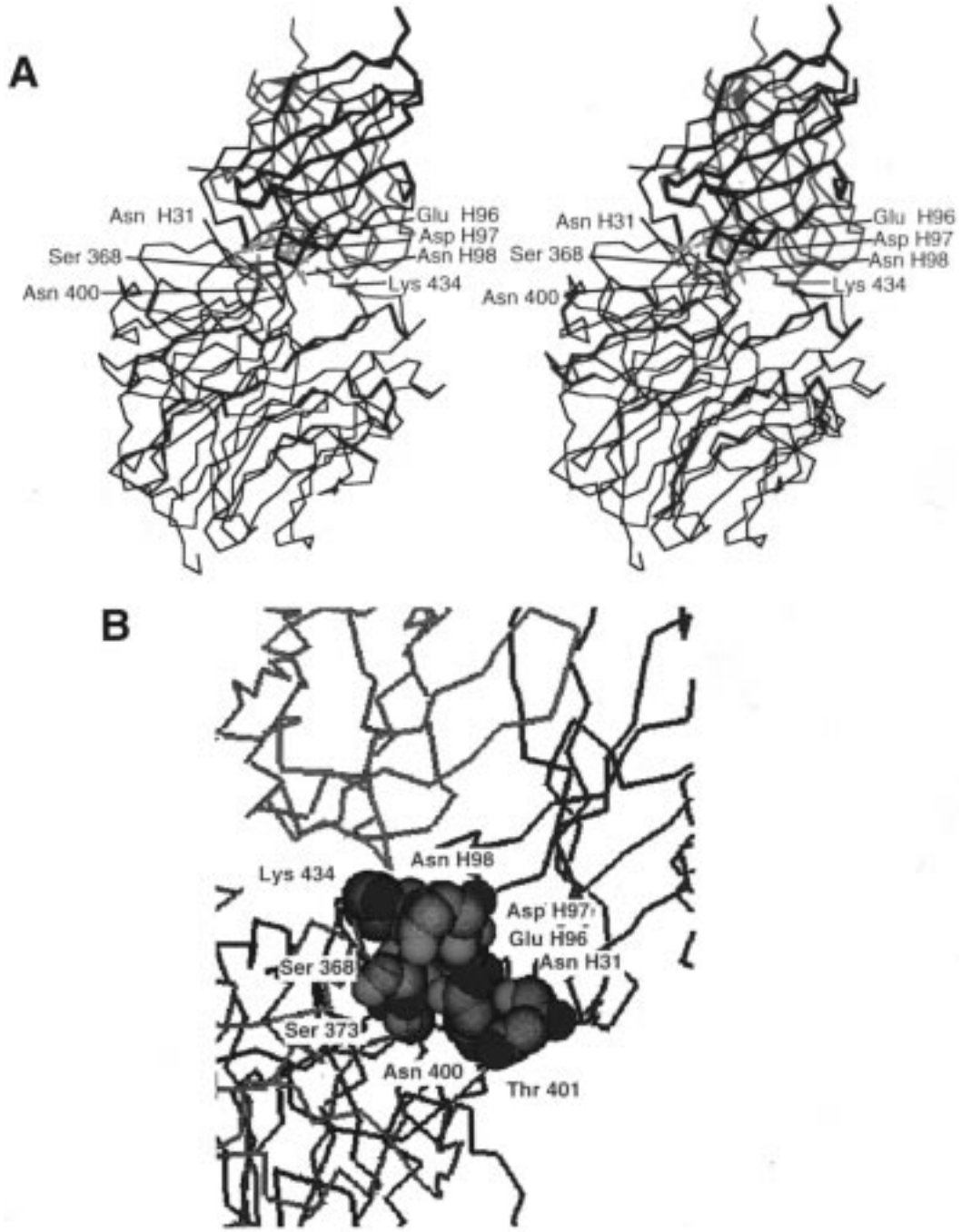

FIGURE 1: (A) Stereoview of interactions at the NC41 Fab−neuraminidase interface. The NA α-carbon chain is gray, and antibody Fv regions are dark blue (heavy chain) and light blue (light chain). The three critical contacts on NA (*4*) are green, with their partners on the Fab that have been mutagenized in this study magenta. (B) Detailed view of the interacting side chains. The antibody and NA chains are colored as they are in panel A, and the complex is rotated about 90° compared to the view in panel A. The side chain atoms are gray (C), red (O), and blue (N). The figures were generated using MacImdad from PDB coordinate file 1NCA (*5*).

purification of the NA (*15*). It contains the HA gene from A/NWS/33 and the NA gene from A/tern/Australia/G70c/75, named A/NWS$_{HA}$-tern/Australia/G70C/75$_{NA}$, subtype H1N9, referred to as NWS-G70c.

Monoclonal Antibodies. Hybridoma cell lines for G70c NA-specific monoclonal antibodies NC41 and NC10 were generously provided by R. G. Webster. Hybridomas were grown in RPMI 1640 (Gibco) with 10% supplemented calf serum (Hyclone) and then transferred to serum-free medium (RPMI 1640 with Nutridoma, Boehringer). Every 2−3 days, the supernatant was harvested and centrifuged (3000 rpm for 15 min in a JA-10 rotor) to remove cellular debris and the antibody purified (*16*). The supernatant was dialyzed against 70% saturated $(NH_4)_2SO_4$ for 1−2 days with frequent mixing. The precipitate was spun down (15 000 rpm for 30 min in a Type 21 rotor), resuspended in a minimum amount of 0.9% NaCl (saline), and dialyzed against saline. The NC41 antibody was then precipitated with 45% saturated $(NH_4)_2SO_4$, again ending with saline dialysis. Alternatively, hybridoma supernatants were purified over a column of Protein A-Sepharose and eluted with 0.1 M sodium citrate at pH 3.9, and fractions were immediately neutralized. The purity of the monoclonal antibodies produced was assessed by SDS−polyacrylamide gel electrophoresis (*17*). Protein

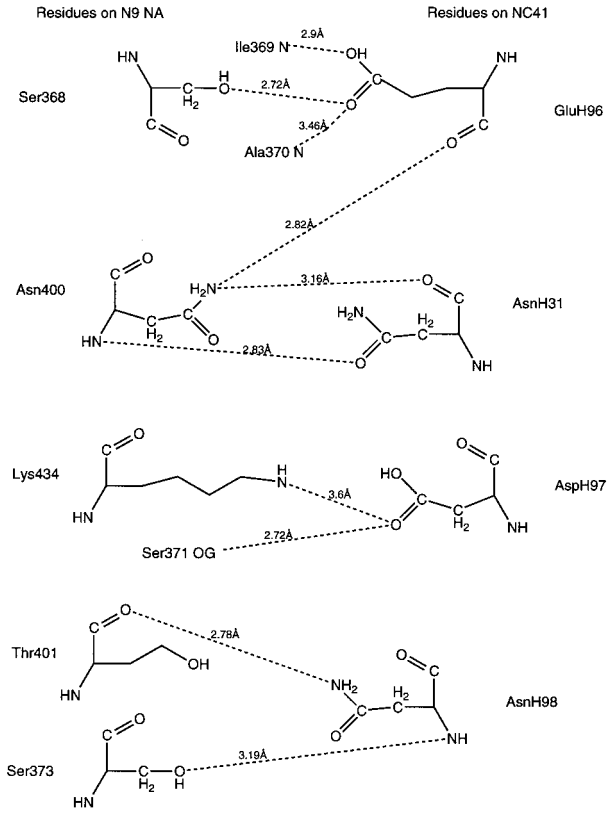

FIGURE 2: Hydrogen bonds and salt bridge between antibody NC41 and G70c NA that involve the side chains of antibody residues N31, E96, D97, and N98. Their partners are NA critical contacts S368, N400, and K434, together with Ser373 and the carbonyl O of T401. Distances are from PDB file 1NCA (*5*).

concentrations of purified antibodies were determined by amino acid analysis at the University of Alabama at Birmingham Protein Sequencing and Peptide Synthesis Core Facility.

Purification of NA Heads. NA is a tetramer comprised of identical globular domains ("head") sitting atop a long thin stalk which attaches the protein to the viral membrane. Because the sialidase activity resides in the tetrameric heads, enzymatically active NA can be separated from the virus by proteolytic cleavage within the stalk region. The procedure was scaled down from the method of Laver (*18*). The NWS-G70c virus was treated with Pronase or proteinase K at a final concentration of 3 mg/mL overnight at room temperature. Residual virus "cores" were removed by centrifugation (30 000 rpm for 1 h with a TLS-55 rotor), and the supernatant was centrifuged at 55 000 rpm (TLS-55 rotor) for 20 h to pellet the NA heads. The NA pellet was dissolved in saline (0.05 mL), and the NA heads were purified by sucrose density gradient centrifugation (5 to 20% sucrose in 0.15 M NaCl, with a SW55 rotor, at 55 000 rpm at 4 °C for 6 h). Fractions containing NA were pooled and dialyzed against saline and then against 70% saturated $(NH_4)_2SO_4$. The precipitated NA heads were spun down, dissolved in a minimum amount of saline, and dialyzed against saline. Purified NA was then pelleted as before (55 000 rpm for 20 h with a TLS-55 rotor) and resuspended in 50−100 μL of saline. Purified NA heads were used in the neuraminidase inhibition assays and fluorescence quenching experiments.

Neuraminidase Activity and Inhibition Assays. The enzyme activity of NA was determined with fetuin as the substrate and the Warren colorimetric assay (*19*). Inhibition of G70c NA activity was determined by preincubation of 50 ng of purified NA with 50 ng of NC41 Ab or 250 ng of MBP−scFv proteins before addition of the substrate.

Extraction and Sequencing of RNA. The sequence of monoclonal antibody NC41 was determined directly from mRNA. Total RNA was extracted from hybridoma cells by the guanidinium/cesium chloride method (*20*). The Sanger dideoxy method, modified for an RNA template, was used for sequencing the RNA (*21*, *22*). The oligonucleotide primers used were 17-mers, which were annealed to the beginning of the constant region of mouse antibody heavy and light chain mRNAs: "gamma" 5′-GGGGCCAGTG-GATAGAC-3′ and "kappa" 5′-TGGATGGTGGGAAGATG-3′.

Cloning of Antibody Genes. The NC41 antibody genes were cloned into pBluescriptSK$^+$ (pBS) (Stratagene). cDNA was generated from total RNA using Invitrogen's First Strand Kit. Polymerase chain reaction (PCR) amplification using sequence-specific primers with 5′-*Eco*RI and 3′-*Sal*I sites allowed directional cloning of individual variable genes into pBS. The 3′-*Sal*I primer also incorporated a termination codon at the end of each variable gene. Thirty cycles of amplification were carried out as follows: 94 °C for 1 min, 40 °C for 1 min, and 72 °C for 2 min. A final extension step at 72 °C for 8 min completed the amplification.

Construction of Antibody Single-Chain Fv. The pBS construct containing the heavy chain variable gene (V_H) was digested with *Eco*RI and *Sca*I for linearization, while the light chain variable gene (V_L) was isolated from pBS by digestion with *Sal*I and *Sca*I. The two genes were ligated into the same vector at the *Sca*I sites and recircularized using a 57-nucleotide linker (AbL) encoding a 15-amino acid peptide $(Gly_4Ser)_3$, with 5′-*Sal*I and 3′-*Eco*RI restriction site overhangs joining the previously cloned individual genes in the order V_H−AbL−V_L. This linker was generated by synthesis (Genosys) of two separate nucleotide strands (51-mers), which were combined in equimolar amounts, annealed at 65 °C for 1 h to form a double-stranded DNA fragment, and then used for the ligation of both genes and the subsequent recircularization of the vector. This forms a single-chain Fv, referred to as "scFv" (*23*). Once constructed in pBS, NC41 scFv was subcloned into the bacterial expression vector pMALp2 (NEB) using *Bam*HI−*Xho*I to *Bam*HI−*Sal*I sites. The sequence was determined using Sequenase (U.S. Biochemicals) with the dideoxy method (*22*).

Mutagenesis of NC41 scFv. Stratagene's Chameleon Double-Stranded Site-Directed Mutagenesis Kit was used for the mutagenesis of CDR residues in the V_H region of NC41 scFv. Mutagenic oligonucleotides (negative sense) are named with the single-letter amino acid code for the original amino acid, its position, and the residue to which it is changed. The bases responsible for the amino acid change are underlined. The oligonucleotides used were as follows: N31Q, 5′-CCAGTTCATTCCATATTGTGTGAAGGTATA-CCC-3′; E96D, 5′-GACTACCGAAGTTATCATCGCCTCT-TGCACAG-3′; D97K, 5′-GAGACTACCGAAGTTTTTCTC-GCCTCTTGCAC-3′; and N98Q, 5′-GAGAGACTACCG-AATTGATCCTCGCCTCTTGC-3′. Colonies were screened by hybridization with radiolabeled mutagenic oligonucleotides and subjected to high-stringency washes to discrimi-

nate between mutants and wild-type plasmids. The NC41 scFv mutant D97K was verified by sequencing double-stranded DNA with Sequenase. An ABI/Prism DNA Sequencer was used to verify mutants N31Q, E96D, and N98Q using dye-labeled terminators.

Expression and Purification of the scFv−MBP Protein. NC41 scFv was subcloned into the expression vector pMalp2 (NEB) at a site within the structural gene for the maltose-binding protein (MBP), producing a fusion product between MBP and the scFv, for inducible expression of the protein in *Escherichia coli*. Insertion of a foreign gene disrupts laczα, allowing blue-white discrimination of plasmid with insert. Expression of the protein is from the ptac promoter; transcription from the promoter is repressed by the Lac repressor until induction by IPTG. Expression as an MBP fusion protein allows detection in Western blots and ELISAs by anti-MBP antisera (NEB) (*24*−*28*). The MBP−laczα fusion protein, which results from expression when no foreign gene has been inserted, was generated as a control. Transformed bacteria were grown at room temperature until A_{600} was 0.5 and then induced to express protein by addition of IPTG to a final concentration of 0.3 mM. To harvest the protein in the periplasmic space, the osmotic shock protocol from the bacterial expression kit (NEB) was used; the fusion protein was also recovered from the pellet after sonication of intact cells. Protein expression was analyzed by silver staining and Western blot analysis of 10% Laemmli gels (*17*). Soluble scFv−MBP protein was purified on an amylose resin affinity column and eluted with 10 mM maltose.

Fluorescence Quenching Assay. Fluorescence quenching of intrinsic tryptophan residues within the NA was used to measure the interaction of NA with NC41 antibody and Fab and provided a preliminary measure of the interaction of scFv proteins with G70c NA. The NC41 epitope on G70c NA includes Trp403, which in unbound NA is exposed to solvent and accessible to excitation by UV irradiation, resulting in the emission of a photon. Addition of antibody or scFv proteins reduces the signal (fluorescence quenching), presumably because Trp403 is now buried in the interface. Experiments were conducted with a Shimadzu R5000U fluorescence spectrophotometer. Wavelengths were set at 280 nm for $\lambda_{excitation}$ and 340 nm for $\lambda_{emission}$. A constant amount of NA in 1 mL of phosphate-buffered saline (pH 7.2) was titrated with scFv protein. After each addition of scFv protein, the sample was equilibrated in the cuvette (room temperature for 2 min) while the mixture was constantly stirred by a magnetic stir bar, before a reading was taken. The percent quenching was calculated after subtracting fluorescence due to antibody alone. This gave the concentration of bound antibody which is the same as the concentration of bound antigen using monomeric molecular weights for each. We calculated K_a using the Scatchard equation (*29*) for each point and averaged these over the central part of the curve.

$$K_a = (\text{fraction of Ab bound})/([\text{total sites}] - [\text{bound Ab}])$$

Enzyme-Linked Immunosorbent Assay (ELISA). Specific binding of NC41 scFv proteins to G70c NA was analyzed by a sandwich ELISA. The wells of a 96-well microtiter plate were coated with NWS-G70c virus containing 143 ng of NA (1:500 dilution, 50 μL per well) and incubated overnight at 4 °C. Following each incubation and subsequent layer of the ELISA, the wells were washed three times with borate-buffered saline. Nonspecific binding was blocked by incubation with 1% calf serum in phosphate-buffered saline for 2 h at room temperature (200 μL per well). The fusion protein or MBP control protein was added in 2-fold serial dilutions (50 μL per well), and the mixture was incubated at room temperature for 3 h. Maltose (50 mM) was included in the diluent to reduce nonspecific binding of MBP, the nature of which is undetermined. Wells were then incubated with rabbit anti-MBP antisera (1:2500 dilution, 50 μL per well) for 3 h at room temperature. Goat anti-rabbit secondary antibody conjugated to horseradish peroxidase (Southern Biotechnology, Birmingham, AL) was added to the wells using a dilution of 1:5000 (50 μL per well), and the mixture incubated at room temperature for 3 h. ABTS substrate, 2,2′-azinobis(3-ethylbenzthiazoline-6-sulfonic acid) (Sigma), was used (100 μL per well) and the absorbance at 414 nm monitored.

Modeling. The structure of NC41 Fab complexed with G70c NA [PDB file 1NCA (*5*)] was used as the framework for modeling the scFv mutants using the program Look (Molecular Applications Group, Palo Alto, CA). Homology modeling was performed using the Encad program within Look, which refines structures with a combination of steepest descents and conjugate gradient energy minimization methods. The output from Encad gives the top 10 most strained interactions (bond lengths, bond angles, torsion angles, ϕ and ψ torsion angles, and nonbonded interactions) for the model before, during, and after refinement. After refinement, the effects of each mutation on hydrogen bond potential, atomic mobility, solvent accessibility, and hydrophobicity were analyzed and compared to those of the wild-type structure.

RESULTS

Expression of NC41 scFv. The nucleotide sequences of NC41 V regions were determined by direct dideoxy sequencing from the RNA, and some regions were confirmed by direct peptide sequencing. Initial experiments for expressing active NC41 or Fab in bacteria or mammalian cells failed, as often happens with antibodies, since they are comprised of two (Fab) or four (Ab) polypeptide chains linked by disulfide bonds. Therefore, we used the approach of Winter to generate a clone that expresses Fv in a single polypeptide with a $(Gly_4Ser)_3$ linker (*23*). Figure 3 shows the nucleotide and deduced amino acid sequences for NC41 scFv, constructed in the order V_H−linker−V_L and inserted into the plasmid pMalp2.

The pMalp2 vector provides a signal for directing MBP fusion products to the periplasmic space. In initial experiments, we found that the yield of fusion protein released by osmotic shock was low, presumably due to a folding problem. The yield was somewhat improved by reducing the growth temperature from 37 °C to room temperature, but much of the protein still remained with the cell fraction after osmotic shock. There was also a considerable level of spontaneous lysis of the outer membrane before osmotic shock. Therefore, the bacteria were lysed by sonication. Much of the MBP−scFv fusion protein was in the fraction pelleted at 8000*g* after sonication, but active scFv could be

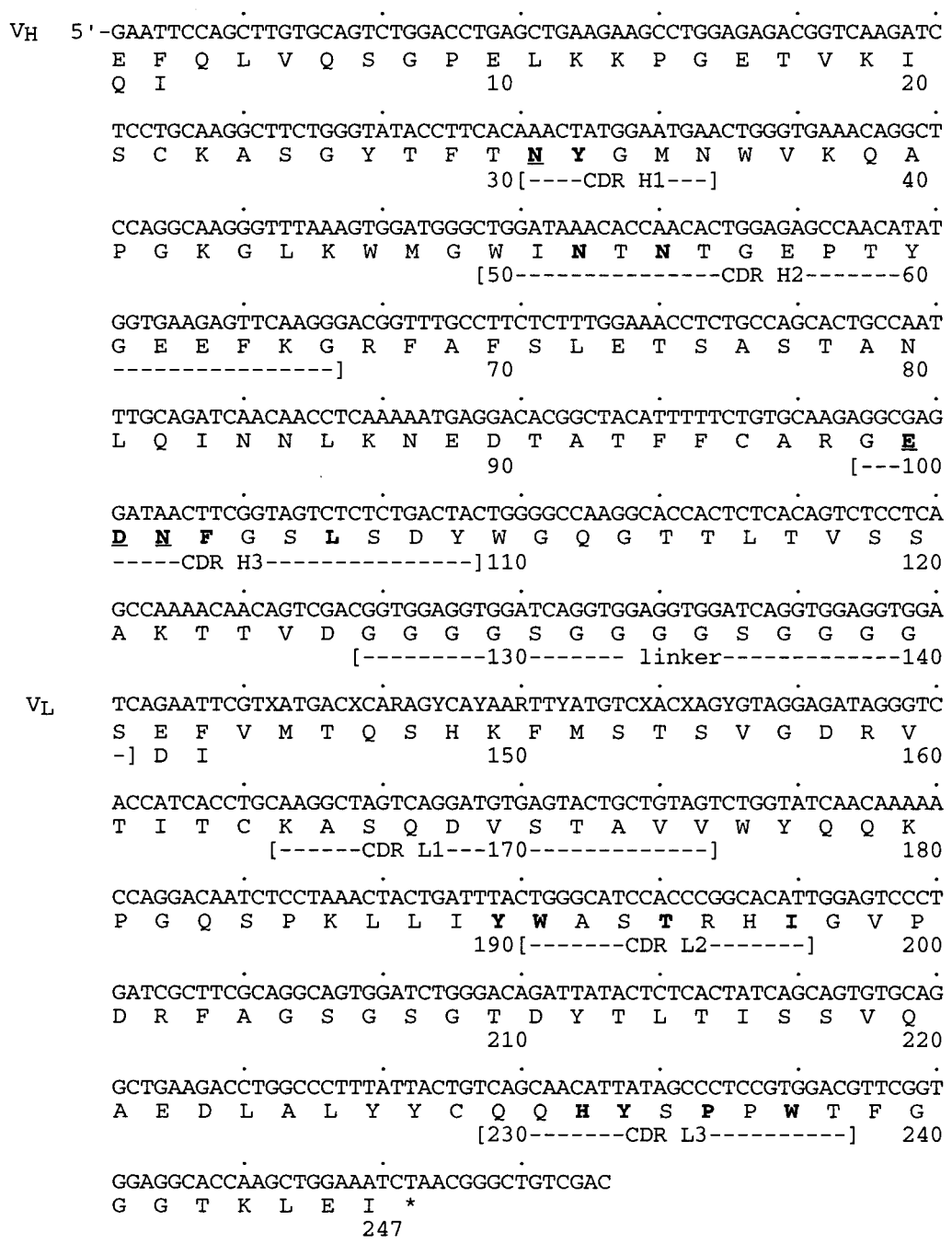

FIGURE 3: Nucleotide and predicted amino acid sequence of the scFv of NC41. The antibody CDRs are marked by dashed lines, as is the $(Gly_4Ser)_3$ peptide linker between V_H and V_L. Residues in contact with G70c NA are bold, and mutated residues are bold and underlined. Incorporation of the 5′-*Eco*RI site during PCR amplification changed V_H residues 1 and 2 from Gln-Ile to Glu-Phe compared to the sequence of NC41 determined from mRNA isolated from the hybridoma line. Similarly, V_L residues 142 and 143 (scFv numbering) have changed from Asp-Ile to Glu-Phe.

recovered by soaking the pellet in buffer (10 mM Tris, 200 mM NaCl, and 1 mM EDTA) overnight.

Figure 4A shows a Western blot of this extract probed with MBP antiserum. The wild-type and mutant scFv proteins are expressed at high levels, but give rise to multiple bands due to premature termination of translation. After adsorption and elution from the amylose column, there is still a background of proteins when the gel is silver stained (Figure 4B). Therefore, for the binding assays, the protein concentrations of the scFv proteins were determined by densitometric analysis of the full-length MBP−scFv band on silver-stained Laemmli gels, with bovine serum albumin as the standard. Since the MBP is N-terminal to the scFv in the fusion protein, the prematurely terminated products will not contribute to the binding. This method was also used to determine the concentration of the NC41 antibody in the ELISAs.

Binding Experiments. We used fluorescence quenching experiments to determine the K_a of the interaction of G70c NA with the NC41 antibody or its Fab in solution phase without any disturbance of the equilibrium of the system (Figure 5). Titrations of G70c NA with NC41 Ab yielded a K_a of 1.2×10^8 M^{-1}. Surprisingly, titration with the Fab gave the same K_a, 1.2×10^8 M^{-1}. The lack of cooperativity with the bivalent antibody is explained by the crystal structure of the NA−Fab complex (*5*). Due to the circular

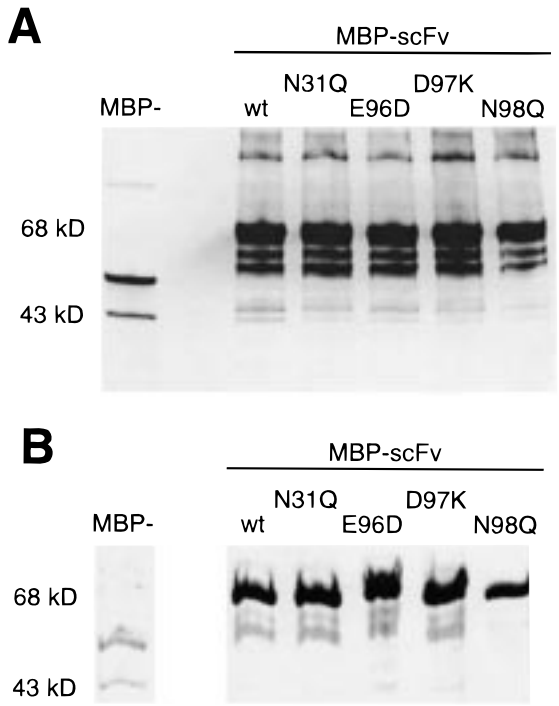

FIGURE 4: (A) Western blot analysis of wild-type and mutant MBP−scFv fusion proteins solubilized from the pellet of the cell lysate. The blot was probed with anti-MBP antiserum and developed with HRP-conjugated antibody and ABTS substrate. (B) Silver-stained gel of wild-type and mutant scFvs after purification.

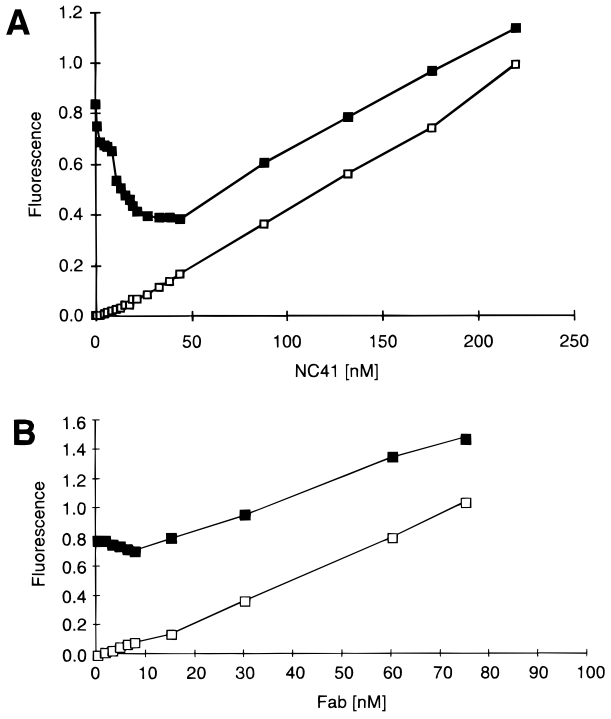

FIGURE 5: Tryptophan fluorescence quenching of G70c NA by NC41 antibody (A) or NC41 Fab (B): (■) curves for NA and antibody and (□) curves for antibody alone.

4-fold symmetry of the NA tetramer and the angle at which the NC41 binds to each monomer, one Ab molecule is physically unable to bind bivalently to a single NA tetramer. Therefore, for whole Ab, Fab, or scFv, binding can be treated as one paratope binding one epitope; binding of the second arm of the Ab to a separate NA molecule is independent of the first.

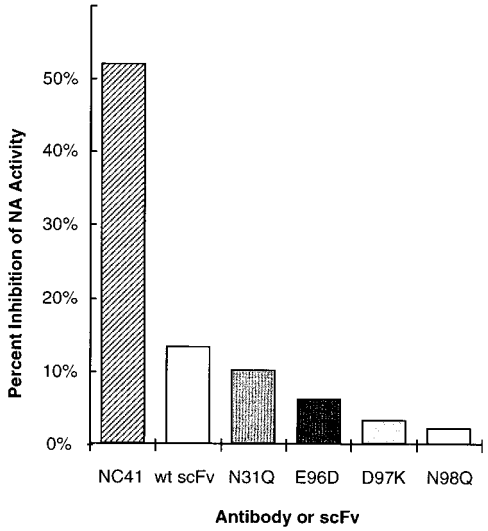

FIGURE 6: Inhibition of G70c NA enzyme activity by NC41 Ab and MBP−scFv proteins. The assays contained the same amount of NA. The molar concentration of MBP−scFv was 5 times that of NC41 Ab, showing that it binds poorly compared to Ab.

To determine whether the MBP−scFv proteins interacted with G70c NA, we first used NA inhibition assays. It was immediately apparent that the wild-type MBP−scFv bound poorly compared to Ab or Fab. Figure 6 shows the results when 50 ng (1 pmol) of purified NA was preincubated with either 50 ng of NC41 Ab (0.7 pmol) or 250 ng of the MBP−scFv protein (3.7 pmol) before addition of substrate. To determine if the poor binding was due to interference by the MBP domain, we cleaved the fusion protein with factor Xa and purified the scFv. Preliminary binding studies indicated that the released scFv was no more active than the fusion protein. The cleavage was slow and inefficient and the yield of scFv too low to measure binding of the mutant scFvs, so we used the MBP−scFv fusion proteins for K_a determinations. An average molecular weight of 68 000 was used for the scFv−MBP proteins, each containing 1 mol of binding sites. The molecular weight of 1 mol of binding sites on whole immunoglobulin is 75 000 (H and L chain). The molecular weight of NA heads is 50 000 per monomer.

We previously showed that inhibition of enzyme activity correlates with binding, but this is not necessarily the case; therefore, we looked to other methods to quantify the effect of the single-site mutations. The results of preliminary fluorescence quenching experiments titrating G70C NA with MBP−scFv and its mutants are shown in Figure 7. The scFv proteins did indeed recognize and bind G70c NA in solution, but there was also some quenching by MBP−laczα, perhaps by interaction with carbohydrates on the NA. When the MBP−laczα is subtracted, the quenching becomes too low for reliable K_a calculation.

These experiments all indicated that the scFv of NC41 binds NA less well than the parent antibody. This restricted the methods available for determining K_a; since the wild-type scFv was less efficient than whole antibody in experiments monitoring quenching of tryptophan fluorescence or enzyme inhibition, the binding-impaired mutant scFvs were so low in activity their effects could not be reliably quantitated. Therefore, we used ELISAs to measure K_a. Purified NA is denatured upon binding plastic, so the plates were coated with the whole virus. The concentration of

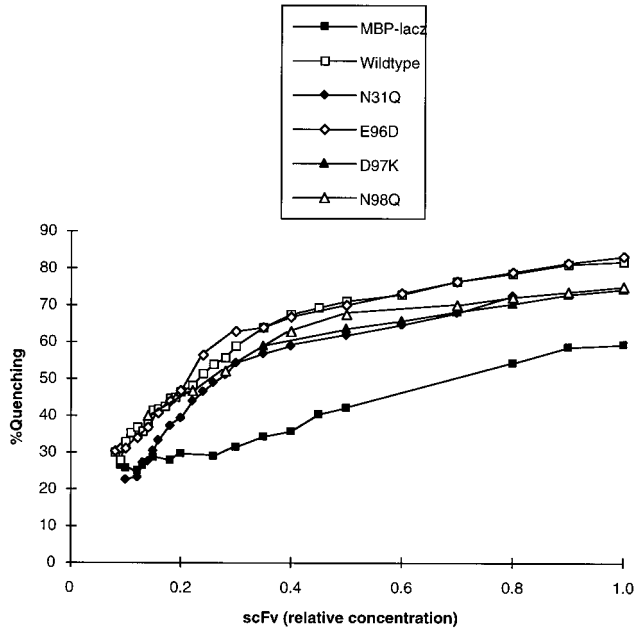

FIGURE 7: Fluorescence quenching of G70c NA by titration with MBP−scFv fusion proteins or MBP−laczα with no scFv attached.

native NA available after the virus was bound to the plate was measured in the well by enzyme activity (*19*) because binding virus to a solid-phase plate decreases the NA available for interaction. Each well was coated with virus containing 143 ng of NA and left overnight at 4 °C, as in the ELISA, and the enzyme activity was compared to that of NA assays in culture tubes. Approximately 42% (60 ng) of the total NA coated was available for interaction with the glycoprotein substrate. This fraction was used as the amount of NA available for interaction with antibody or scFv; we have previously shown this to be the case (*4*). As with the preliminary fluorescence quenching experiments, MBP−laczα interacted with NA in the ELISAs, to a lesser degree than the MBP−scFv proteins, so these values were subtracted before K_as were calculated.

Binding curves are shown in Figure 8, which depicts the binding of wild-type scFv and each mutant scFv as a percentage of its maximum A_{414}. The K_a can be estimated from these binding curves since it is the reciprocal of the dissociation constant (K_d), which is the antibody concentration at which 50% of the NA is bound. For a more reliable determination, we calculated the K_a for each mutant MBP−scFv from the binding equation applied to each point of the binding curve averaged over three determinations. The results are shown in Table 2. The first column lists the K_as estimated from the binding curves (Figure 8). The second column lists the K_as calculated from the binding equation. The K_a for NC41 Ab binding to G70c NA is 4×10^8 M^{-1}; K_as for the scFv proteins were considerably lower, in the 10^6-10^7 M^{-1} range, as was seen in fluorescence quenching and NA inhibition assays. The K_a determined for NC41 binding to G70c NA in an ELISA is close to that determined in the fluorescence quenching experiments, so although the ELISA involves washing and other steps where Ab might dissociate, it apparently does not. The possibility that the loss of antibody during ELISA is offset by an increased K_a in the solid phase remains, so despite the excellent agreement between the methods, the K_as determined by the ELISA should be considered relative rather than absolute. The order

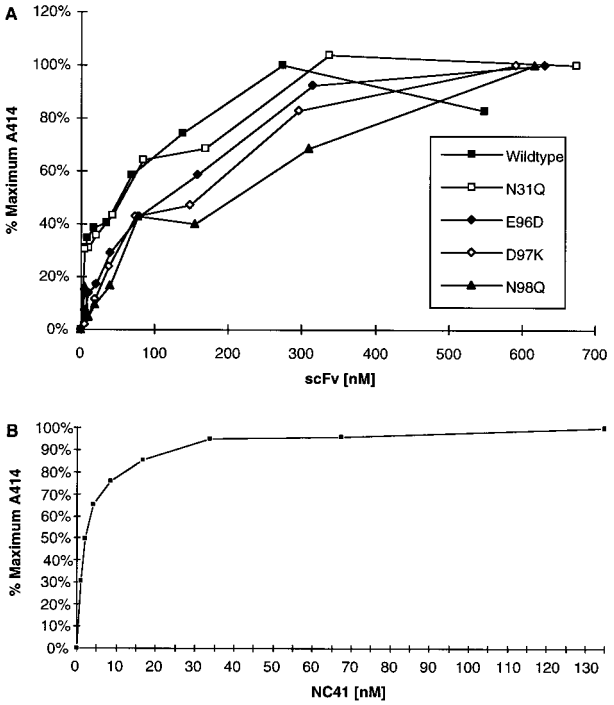

FIGURE 8: (A) Binding curves for purified wild-type and mutant MBP−scFv fusion proteins. A fixed amount of G70c NA was reacted with varying amounts of MBP−scFv in an ELISA. The data are expressed as a percentage of the maximum absorbance at 414 nm. The degree of binding is determined by the concentration at which 50% of the NA is bound. Each data point is the average of three determinations. The errors are not plotted as error bars or curve fits but are calculated as described in Table 2. (B) Binding curve for NC41 Ab in the same assay.

Table 2: K_as of the NC41 Antibody and Wild-Type and Mutant scFvs Determined with an ELISA[a]

	K_a[b] (M^{-1})	K_a[c] (M^{-1})
NC41 Ab	50×10^7	$(38 \pm 7) \times 10^7$
wild-type scFv	2.1×10^7	$(2.0 \pm 0.1) \times 10^7$
N31Q scFv	1.9×10^7	$(2.0 \pm 0.4) \times 10^7$
E96D scFv	0.9×10^7	$(1.3 \pm 0.3) \times 10^7$
D97K scFv	0.7×10^7	$(0.6 \pm 0.2) \times 10^7$
N98Q scFv	0.6×10^7	$(0.8 \pm 0.1) \times 10^7$

[a] Using fluorescence quenching, the K_a for NC41 Ab was determined to be 12×10^7 M^{-1}; for the NC41 Fab, the K_a is the same, 12×10^7 M^{-1}. [b] Estimated from the binding curves (Figure 8). [c] Determined from the binding equation K_a = [bound NA]/[free NA][free Ab] for each point and averaged.

of binding was as follows: NC41 Ab ≫ wild-type scFv = N31Q > E96D > N98Q > D97K.

Structural Interpretation of Binding Results. To understand the structural basis of the binding results, we used the program Encad (within the Look package) to homology model each mutation individually from the wild-type structure coordinates 1NCA (*5*). The effect of each mutation on hydrogen bond potential, atomic mobility, solvent accessibility, and hydrophobicity was evaluated by a combination of steepest descents and conjugate gradient energy minimization methods. Before minimization, the mutant side chains did not fit into the wild-type Fab−NA complex structure as shown by highly strained interactions. By the time full refinement is completed, the mutant residues are no longer within the 10 most strained interactions, indicating that these mutations can be accommodated within the antibody−antigen

Table 3: Atomic Mobility, Hydrophobicity, and Solvent Accessibility in NC41 and Modeled in scFv Mutants

NC41	atom	*B* factor[a] (Å^2)	highest in residue	scFv	atom	highest in residue
Asn31	Nδ2	37−39	yes	N31Q	Nε2	yes
	Oε1	37−39	yes		Oε1	no
	O	25−26	no		O	no
Glu96	Oε1	13.5−14	yes	E96D	Oδ1	yes
	Oε2	10−10.5	no		Oδ2	no
	O	13.5−14	yes		O	no
Asp97	Oδ1	16.0−16.3	yes	D97K	Nζ	yes
Asn98	Nδ2	3.2−3.8	no	N98Q	Nε2	yes
	N	9.9−10.5	yes		N	no
	Oδ1	3.2−3.8	no		Oε1	no

residue	hydrophobicity[b]	% burial[c]	residue	hydrophobicity	% burial
Asn31	−0.08	78	N31Q	−0.17 to −0.16	69−71
Glu96	0.31	93	E96D	0.20−0.24	89−90
Asp97	0.21	92	D97K	0.36−0.37	94−95
Asn98	−0.08	91	N98Q	−0.02 to 0.0	92−94

[a] *B* factors from coordinate file 1NCA; higher values indicate flexibility, and lower values indicate constrained atoms. [b] Hydrophobicity of the residues determined by Look (*43*). [c] Solvent accessibility quantified by Look and expressed as a fraction of each residue's surface.

interface. This is consistent with the ELISA results showing that all mutants bind to some extent. Table 3 lists atomic mobilities, hydrophobicities, and solvent accessibilities of the wild type and each mutant side chain. The refined models show very little difference in these properties between the wild type and mutants, further indicating that the mutations can be tolerated in the Ab−Ag complex.

Table 4 lists the hydrogen bond potentials of the scFv mutants. N31Q maintains both hydrogen bonds with critical contact Asn400. Of its four hydrogen bonds, E96D retains those to critical contact Ser368 and Ala370, while losing the bonds to Ile369 and Asn400. D97K loses both the salt bridge with critical contact Lys434 and the hydrogen bond with Ser371, but forms a new hydrogen bond with Ser373. N98Q loses its hydrogen bond to Thr401, maintains its hydrogen bond with Ser373, and forms a new hydrogen bond with Trp403.

The reduction in binding of all the antibody mutants was far less dramatic than the abrogation of binding seen when NA contact residues were mutated (*4*). To understand the basis of the difference, the critical contact residue mutants of the NA were modeled and refined using Look in the same manner that was used for the scFv mutants. The resulting hydrogen bonding patterns are shown in Table 5. S368T loses its hydrogen bond with Glu96. N400Q loses both hydrogen bonds from its side chain to Asn31 and Glu96, while maintaining its main chain hydrogen bond to Asn31. K434D loses its salt link with Asp97. Thus, the predicted structural effects of these NA mutations are larger than those for the antibody mutations, consistent with the experimental results. Our results indicate that the NA epitope is highly defined but can interact with variant antibodies like those encountered during antibody maturation in vivo.

DISCUSSION

The purpose of our study was to determine which residues on the antibody are the most important in the binding interaction. Novotny and co-workers (*30*, *31*) first proposed the concept of "energetic epitopes", based on energy calculations using lysozyme−Fab crystal structures. They hypothesized that a small number of amino acid residues within the epitope contribute most of the binding energy. We previously provided experimental confirmation of this for the NA antigen by showing that, of 19 contacting amino acids on G70c NA, only three, centered within the epitope, are critical to its interaction with antibody NC41 (*4*). The results could be related to biology, since these three amino acid residues were the only sites of amino acid changes in escape mutants except for a bulky Ser → Tyr substitution (*11*, *12*). Energy calculations for the G70c NA−Fab complex indicated a centrally located energetic epitope. Calculated ΔG values

Table 4: Hydrogen Bonds[a] in the Wild-Type Complex and Predicted for the scFv Mutants

NC41 Ab	atom	NA	atom	distance (Å)	scFv	atom	distance (Å)	H bond	binds NA
Asn31	Oδ1	Asn400	N	2.83	Gln31	Oε1	2.95	yes	yes
	O		Nδ2	3.16		O	3.21	yes	
Glu96	Oε1	Ser368	Oγ	2.72	Asp96	Oδ1	2.83	yes	yes
	Oε1	Ala370	N	3.46		Oδ1	3.34	yes	
	Oε2	Ile369	N	2.95		Oδ2	5.77	no	
	O	Asn400	Nδ2	2.82		O	3.60	no	
Asp97	Oδ1	Lys434	Nζ	3.61 charged	Lys97			no	less
	Oδ2	Ser371	Oγ	2.72				no	
		Ser373	Oγ			Nζ	3.53	yes[b]	
Asn98	Nδ2	Thr401	O	2.78	Gln98	Nε2	3.71	no	less
	N	Ser373	Oγ	3.19		N	3.45	yes	
	Oδ1	Trp403	N			Oε1	2.94	yes[b]	

[a] Defined by Look on the basis of distance and angle. [b] Predicted H bonds not present in the wild-type complex.

Table 5: Hydrogen Bonds in the Wild-Type Complex and Predicted for NA Mutants

G70c NA	atom	NC41 Ab	atom	distance (Å)	NA mutant[a]	atom	distance (Å)	H bond[b]	binds NC41
Ser368	Oγ	Glu96	Oε1	2.72	Thr368	Oδ	3.31	no	no
Asn400	N	Asn31	Oδ1	2.83	Gln400	N	2.87	yes	no
	Nδ2	Asn31	O	3.16		Nε2	4.21	no	
	Nδ2	Glu96	O	2.82		Nε2	2.91	no	
Lys434	Nζ	Asp97	Oδ1	3.61 charged	Asp434	Oδ1		no	no

[a] Reference *4*. [b] Defined by Look.

for the contributions of individual side chains (*32*) correlated well with the experimental data (*4*) in that NA residues with a ΔG value of less than -1 kcal/mol were also the residues at which mutation caused a reduction or loss in binding.

To determine if there were corresponding critical contacts on the antibody, we made mutations in the four residues that (a) are partners with NA critical contacts and (b) involve side chain rather than just main chain interactions. The residues chosen for mutagenesis were those that have the greatest potential for comprising critical contacts within the paratope. These are Asn31 in CDR H1 and Glu96, Asp97, and Asn98 in CDR H3. These four residues are responsible for nine of the twelve hydrogen bonds and the only salt link between NC41 and G70c NA. On the basis of the energy calculations, these residues should contribute most to the binding energy, with ΔG values ranging from -2 to -5 kcal/mol (*32*). Asn is more frequently found in CDRs than in framework regions (*33*), and Asn residues are seen to contribute more to the interaction between NC41 and G70c NA than any other residue. There are four Asn residues on each protein that make five of the twelve hydrogen bonds; Asn can act as both a hydrogen bond donor and acceptor. Asn residues account for 15 contacts out of 104 for G70c NA with a 159 Å^2 buried surface area contributing to the total 899 Å^2 and for 35 contacts out of 104 for NC41 accounting for 143 Å^2 out of the total of 916 Å^2 of buried surface area (*5*).

The G70c NA residues critical to its interaction with NC41 are Ser368, Asn400, and Lys434 (*4*), which have multiple contacts with the antibody (*5*). We tested these multiple interactions by making conservative amino acid substitutions at antibody H chain residues Asn31, Glu96, Asp97, and Asn98. The effect of these changes on binding was measured with an ELISA. The wild-type scFv bound 1 order of magnitude less than whole antibody, presumably due to its increased flexibility (decreased stability) and perhaps interference from the linking peptide. Despite this flexibility and the reduced affinity of the scFv proteins relative to that of the antibody, the interactions with G70c NA were strong enough to detect and quantify the differences in binding due to a single amino acid change. Modeling studies indicate that the structural effects of the scFv mutations on the NC41−NA interaction are significantly less than those of equivalent mutations on the NA, consistent with the narrow range of K_as when antibody mutants are assayed compared to the dramatically lower K_as when the mutations are in the NA.

For the following discussion of the interactions between NC41 and G70c, refer to Figure 2 and Tables 4 and 5.

Heavy chain CDR1 residue Asn31 makes two hydrogen bonds with NA critical contact Asn400: one through its main chain O atom to side chain Nδ2 and the other from its side chain Oδ1 atom to the main chain N atom (*5*). Substitution of Gln for Asn (N31Q) has no effect on binding; the K_as for the wild type and N31Q scFv were identical at 2×10^7 M^{-1}. The ability of N31Q to retain binding at wild-type levels demonstrates that the critical contacts are from the Nδ2 of NA residue 400 to the main chain carbonyl O's of Asn31 and/or Glu96 and that the side chain of Asn31 is less important; i.e., its hydrogen bond to the main chain N either is dispensable or can still be formed from the shorter side chain. Modeling studies indicate that N31Q can form both hydrogen bonds. The reciprocal mutation in NA, substitution of Gln at residue 400 (N400Q), caused a complete loss of binding with NC41 (*4*). Modeling of this mutation shows a loss of both hydrogen bonds from its side chain Nδ2 to the O's of Asn31 and Glu96, consistent with the experimental result of undetectable binding.

NC41 residue Glu96 makes a hydrogen bond through its side chain Oϵ1 to the side chain Oγ of Ser368 of G70c NA. Glu96 forms three other hydrogen bonds with NA: one from the side chain Oϵ1 to the main chain N of Ala370, one from the side chain Oϵ2 to the main chain N of Ile369, and one from the main chain O to the side chain Nδ1 of Asn400. Substitution of Asp for Glu maintains the charge characteristics of the side chain, but the side chain is shorter and slightly more rigid. Alteration of the side chain−side chain interaction with critical contact residue Ser368 could potentially cause a drastic reduction in binding; however, the K_a for the interaction of E96D with G70c NA showed only a 2-fold reduction compared to that of wild-type scFv. Homology modeling indicates that the hydrogen bonds with Ser368 and Ala370 are maintained, while those with Ile369 and Asn400 are not. The ability to maintain the hydrogen bond through its side chain Oδ1 to the Oγ of critical contact Ser368 allows mutant E96D to maintain binding to G70c NA. NC41 residue Asp97 makes one hydrogen bond with NA through its side chain Oδ1 to the side chain Oγ of Ser371 and one salt link through Oδ1 to the Nζ of Lys434. Substitution of Asp by Lys in this context is a drastic, nonconservative change that substantially increases the length of the side chain and also reverses the charge from negative to positive. This substitution was expected to abolish binding with G70c NA due to disruption of the salt bridge, and because a reciprocal substitution in NA abolished the binding (*4*). The K_a for D97K is the lowest of the values for the four scFv mutants at 6×10^6 M^{-1}, but there is still only a 3−4-fold reduction in binding compared to that of wild-type scFv. Modeling of D97K shows that the side chain can fit within the interface, with Nζ able to form a hydrogen bond with Oγ of Ser373. Modeling of the reciprocal mutation in NA (K434D) shows that the shorter side chain points downward toward NA and away from the interface, unable to form any type of binding interaction with NC41, again consistent with previous experimental results (*4*).

NC41 H chain residue Asn98 forms two hydrogen bond interactions with NA. The main chain N forms a hydrogen bond with Oγ of Ser373, and the side chain Nδ2 forms a hydrogen bond with the main chain O of Thr401. A comparison of Fab-complexed and uncomplexed NA shows a shift of 0.5 Å in the backbone of Thr401, attributed to the proximity of the side chain of Asn98, which sits between Thr401 and Trp403 (*5*). The substitution from Asn to Gln maintains the chemical side chain characteristics. N98Q showed a 2.5-fold reduction in binding (8×10^6 M^{-1}), compared to that of wild-type scFv. Modeling of N98Q shows a loss of the hydrogen bond to Thr401, with the formation of a new hydrogen bond to the N of Trp403. N98Q maintains binding due to the hydrogen bonds with Ser373 and Trp403.

A striking feature of our data is the narrow range of K_as for the wild type and mutants, as seen with an ELISA. The scFv is less stable than the whole antibody, resulting in a 20-fold reduction in K_a. We initially thought that the inherent flexibility of the scFv allows mutant D97K to form new inter-

actions with NA and thus maintain a reduced level of binding; however, our modeling studies show that a new hydrogen bond forms even when the model is based on the Fab structure with no allowance for increased flexibility. There is no new hydrogen bond seen when the corresponding mutation in the NA is modeled. Our binding assay was necessarily different from the immunoprecipitation assays used for the NA mutants because the scFv has no Fc for binding protein A, so we cannot directly compare the results with those of mutating the NA (*4*); however, the 3-fold reduction in binding by our antibody mutant K97D measured with an ELISA is clearly less than the >90% reduction of binding by NA mutant K434D measured by immunoprecipitation.

We conclude that the NC41 antibody paratope better accommodates change than its epitope on the NA. This makes biological sense in that the influenza virus uses single changes in epitopes to escape from antibody neutralization, while antibody molecules are designed to evolve, with selection for sequence changes that increase their affinity.

ACKNOWLEDGMENT

We thank Dr. Robert Webster (St. Jude's Hospital) for providing the NC41 hybridoma line, Dr. Susan Hollingshead and her staff at the University of Alabama at Birmingham for the DNA sequencing, Dr. Herb Cheung for assistance with the fluorescence quenching calculations, and Dr. Jacqueline Nuss Parker for many helpful discussions.

REFERENCES

1. CDC (1995) *Morbidity and Mortality Weekly Report 44*, 535−537.
2. Liu, C., Eichelberger, M. C., Compans, R. W., and Air, G. M. (1995) *J. Virol. 69*, 1099−1106.
3. Palese, P., Tobita, K., Ueda, M., and Compans, R. W. (1974) *Virology 61*, 397−410.
4. Nuss, J. M., Whitaker, P. B., and Air, G. M. (1993) *Proteins: Struct., Funct., Genet. 15*, 121−132.
5. Tulip, W. R., Varghese, J. N., Laver, W. G., Webster, R. G., and Colman, P. M. (1992) *J. Mol. Biol. 227*, 122−148.
6. Kabat, E. A., Wu, T. T., Perry, H. M., Gottesman, K. S., and Foeller, C. (1991) *Sequences of proteins of immunological interest*, 5th ed., U.S. Department of Health and Human Services, Public Health Service, National Institutes of Health, Bethesda, MD.
7. Chothia, C., Lesk, A. M., Tramontano, A., Levitt, M., Smith-Gill, S. J., Air, G. M., Sheriff, S., Padlan, E. A., Davies, D., Tulip, W. R., Colman, P. M., Spinelli, S., Alzari, P. M., and Poljak, R. J. (1990) *Nature 342*, 877−883.
8. Wu, T. T., Johnson, G., and Kabat, E. A. (1993) *Proteins: Struct., Funct., Genet. 16*, 1−7.
9. Bizebard, T., Gigant, B., Rigolet, P., Rasmussen, B., Diat, O., Bosecke, P., Wharton, S. A., Skehel, J. J., and Knossow, M. (1995) *Nature 376*, 92−94.
10. Tulip, W. R., Varghese, J. N., Webster, R. G., Laver, W. G., and Colman, P. M. (1992) *J. Mol. Biol. 227*, 149−159.
11. Webster, R. G., Air, G. M., Metzger, D. W., Colman, P. M., Varghese, J. N., Baker, A. T., and Laver, W. G. (1987) *J. Virol. 61*, 2910−2916.
12. Air, G. M., Laver, W. G., and Webster, R. G. (1990) *J. Virol. 64*, 5797−5803.
13. Laver, W. G., Air, G. M., Webster, R. G., and Smith-Gill, S. J. (1990) *Cell 61*, 553−556.
14. Tulip, W. R., Varghese, J. N., Webster, R. G., Air, G. M., Laver, W. G., and Colman, P. M. (1989) *Cold Spring Harbor Symp. Quant. Biol. 54*, 257−263.
15. Laver, W. G., Colman, P. M., Webster, R. G., Hinshaw, V. S., and Air, G. M. (1984) *Virology 137*, 314−323.
16. Laver, W. G., Webster, R. G., and Tulloch, P. A. (1985) in *Immune Recognition of Protein Antigens* (Laver, W. G., and Air, G. M., Eds.) pp 145−149, Cold Spring Harbor Laboratory Press, Plainview, NY.
17. Laemmli, U. K. (1970) *Nature 227*, 680−685.
18. Laver, W. G. (1978) *Virology 86*, 78−87.
19. Aymard-Henry, M., Coleman, M. T., Dowdle, W. R., Laver, W. G., Schild, G. C., and Webster, R. G. (1973) *Bull. W. H. O. 48*, 199−202.
20. Sambrook, J., Fritsch, E. F., and Maniatis, T. (1989) *Molecular Cloning: A Laboratory Manual.*, 2nd ed., Cold Spring Harbor Laboratory Press, Plainview, NY.
21. Air, G. M. (1979) *Virology 97*, 468−472.
22. Sanger, F., Nicklen, S., and Coulson, A. R. (1977) *Proc. Natl. Acad. Sci. U.S.A. 74*, 5463−5467.
23. Orlandi, R., Gussow, D. H., Jones, P. T., and Winter, G. (1989) *Proc. Natl. Acad. Sci. U.S.A. 86*, 3833−3837.
24. Amann, E., and Brosius, J. (1985) *Gene 40*, 183−190.
25. Duplay, P., Bedouelle, H., Fowler, A., Zabin, I., Saurin, W., and Hofnung, M. (1984) *J. Biol. Chem. 259*, 10606−10613.
26. Guan, C., Li, P., Riggs, P. D., and Inouye, H. (1987) *Gene 67*, 21−30.
27. Kellerman, O. K., and Ferenci, T. (1982) *Methods Enzymol. 90*, 459−463.
28. Maina, C. V., Riggs, P. D., Grandea, A. G. I., Slatko, B. E., Moran, L. S., Tagliamonte, J. A., McReynolds, L. A., and Guan, C. (1988) *Gene 74*, 365−373.
29. Scatchard, G. (1949) *Ann. N.Y. Acad. Sci. 51*, 660−672.
30. Novotny, J. (1991) *Mol. Immunol. 28*, 201−207.
31. Novotny, J., Bruccoleri, R. E., and Saul, F. A. (1989) *Biochemistry 28*, 4735−4749.
32. Tulip, W. R., Harley, V. R., Webster, R. G., and Novotny, J. (1994) *Biochemistry 33*, 7986−7997.
33. Padlan, E. A. (1990) *Proteins 7*, 112−124.
34. Davies, D. R., Sheriff, S., and Padlan, E. A. (1988) *J. Biol. Chem. 263*, 10541−10544.
35. Fischmann, T. O., Bentley, G. A., Bhat, T. N., Boulet, F., Mariuzza, R. A., Phillips, S. E. V., Tello, D., and Poljak, R. J. (1991) *J. Biol. Chem. 266*, 12915−12920.
36. Sheriff, S., Silverton, E. W., Padlan, E. A., Cohen, G. H., Smith-Gill, S. J., Finzel, B. C., and Davies, D. R. (1987) *Proc. Natl. Acad. Sci. U.S.A. 84*, 8075−8079.
37. Padlan, E. A., Silverton, E. W., Sheriff, S., Cohen, G. H., Smith-Gill, S. J., and Davies, D. R. (1989) *Proc. Natl. Acad. Sci. U.S.A. 86*, 5938−5942.
38. Chitarra, V., Alzari, P. M., Bentley, G. A., Bhat, T. N., Eiselé, J.-L., Houdusse, A., Lescar, J., Souchon, H., and Poljak, R. J. (1993) *Proc. Natl. Acad. Sci. U.S.A. 90*, 7711−7715.
39. Fields, B. A., Goldbaum, F. A., Ysern, X., Poljak, R. J., and Mariuzza, R. A. (1995) *Nature 374*, 739−742.
40. Bentley, G. A., Boulot, G., Riottot, M. M., and Poljak, R. J. (1990) *Nature 348*, 254−257.
41. Bossart-Whitaker, P., Chang, C. Y., Novotny, J., Benjamin, D. C., and Sheriff, S. (1995) *J. Mol. Biol. 253*, 559−575.
42. Malby, R. L., Tulip, W. R., Harley, V. R., McKimm-Breschkin, J. L., Laver, W. G., Webster, R. G., and Colman, P. M. (1994) *Structure 2*, 733−746.
43. Nozaki, Y., and Tanford, C. (1971) *J. Biol. Chem. 246*, 2211−2217.

BI9802059